10/20, 10/10, and 10/5 systems revisited: Their validity as relative head-surface-based positioning systems ☆

Valer Jurcak[1], Daisuke Tsuzuki[1], and Ippeita Dan*

Sensory and Cognitive Food Science Laboratory, National Food Research Institute, 2-1-12 Kannondai, Tsukuba 305-8642, Japan

With the advent of multi-channel EEG hardware systems and the concurrent development of topographic and tomographic signal source localization methods, the international 10/20 system, a standard system for electrode positioning with 21 electrodes, was extended to higher density electrode settings such as 10/10 and 10/5 systems, allowing more than 300 electrode positions. However, their effectiveness as relative head-surface-based positioning systems has not been examined. We previously developed a virtual 10/20 measurement algorithm that can analyze any structural MR head and brain image. Extending this method to the virtual 10/10 and 10/5 measurement algorithms, we analyzed the MR images of 17 healthy subjects. The acquired scalp positions of the 10/10 and 10/5 systems were normalized to the Montreal Neurological Institute (MNI) stereotactic coordinates and their spatial variability was assessed. We described and examined the effects of spatial variability due to the selection of positioning systems and landmark placement strategies. As long as a detailed rule for a particular system was provided, it yielded precise landmark positions on the scalp. Moreover, we evaluated the effective spatial resolution of 329 scalp landmark positions of the 10/5 system for multi-subject studies. As long as a detailed rule for landmark setting was provided, 241 scalp positions could be set effectively when there was no overlapping of two neighboring positions. Importantly, 10/10 positions could be well separated on a scalp without overlapping. This study presents a referential framework for establishing the effective spatial resolutions of 10/20, 10/10, and 10/5 systems as relative head-surface-based positioning systems.

Introduction

The international 10/20 system has stood as the de-facto standard for electrode placement used in electroencephalography (EEG) for half a century. This system describes head surface locations via relative distances between cranial landmarks over the head surface. The primary purpose of the 10/20 system (Jasper, 1958) was to provide a reproducible method for placing a relatively small number (typically 21) of EEG electrodes over different studies, and there was little need for high spatial resolution and accurate electrode placement.

With the advent of multi-channel EEG hardware systems and the concurrent development of topographic methods and tomographic signal source localization methods, there was an increased need for extending the 10/20 system to higher density electrode settings. Therefore, the 10/10 system, an extension to the original 10/20 system with a higher channel density of 81, was proposed (Chatrian et al., 1985; see Supplementary material 2 for details). After some arguments on the nomenclature of electrode positions (Nuwer, 1987), its modified form has also been accepted as a standard of the American Clinical Neurophysiology Society (ACNS; former American Electroencephalographic Society; Klem et al., 1999; American Electroencephalographic Society, 1994) and the International Federation of Clinical Neurophysiology (IFCN; former International Federation of Societies for Electroencephalography and Clinical Neurophysiology; Nuwer et al., 1998). However, high-end users sought even higher density electrode settings. 128 channel systems are now a common commercial choice, and even 256 channel EEG systems are commercially available (Suarez et al., 2000). Thus, Oostenveld and Praamstra (2001) logically extended the 10/10 system to the 10/5 system, enabling the use of more than 300 electrode locations (320 were described explicitly).

In the meantime, the 10/20 system's primary use began to shift from simply providing guidance for placing EEG electrodes to being used for direct positional guidance for newly developing transcranial neuroimaging techniques, near-infrared spectroscopy (NIRS; Okamoto et al., 2004a,b), and transcranial magnetic stimulation (TMS; Herwig et al., 2003). Use of the 10/20 system allows reproducible probe or coil settings on scalps of multiple subjects.

Moreover, the 10/20 system serves as the standard cranial landmarks for mediating probabilistic registration (Okamoto et al., 2004a; Okamoto and Dan, 2005; Singh et al., 2005; Tsuzuki et al., 2006). In a series of previous papers, we established a method to probabilistically register any given scalp position to the corresponding scalp or cortical point in standard stereotaxic brain coordinate systems such as MNI (Montreal Neurological Institute) and Talairach systems without the use of MR images of a subject. Since these stereotaxic brain coordinates serve as the common spatial platform for data presentation of conventional tomographic neuroimaging techniques including fMRI and PET (Collins et al., 1994; Talairach and Tournoux, 1988; reviewed in Brett et al., 2002), the registration of stand-alone multi-subject fNIRS and TMS data to a brain template in the MNI standard coordinate system facilitates both intra- and inter-modal data sharing within the neuroimaging community. Therefore, the 10/20 system has been gaining importance as a standard relative head-surface-based positioning method for various transcranial brain mapping methods.

However, it is also true that the original 10/20 system has not been equipped as a versatile system to fully support such unexpected applications. In the process of developing high density settings, the 10/20-derived systems have been mainly appreciated as methods to increase spatial resolution for EEG studies, where more densely positioned electrodes are proven to be effective in increasing the spatial resolution when the three-dimensional signal source estimation is applied (Pascual-Marqui et al., 2002). Meanwhile its aspect as a relative head-surface-based positioning system has not been examined well. In particular, how effectively high-resolution derivatives of the 10/20 system can separate each cranial landmark, which is especially important for head-surface-based positional estimation in TMS and NIRS, still remains unknown. Therefore, we will evaluate the effective spatial resolution of the 10/20, 10/10, and 10/5 systems for multi-subject studies. We will focus on two sources of variability. First, definitions of landmark placement in the original 10/20 system by Jasper (1958) are ambiguous, and this results in different interpretations among experimenters and variability among studies. Second, even if a fixed definition of landmark placement is used, scalp and cortical anatomies are different among subjects and this results in inter-subject variability.

To evaluate variability, we performed virtual 10/20, 10/10, and 10/5 measurements on MR images that we described previously. Subsequently, we transformed all the scalp data to MNI space and statistically assessed the spatial variability. In so doing, we sought to assess the potential of 10/20, 10/10, and 10/5 systems as relative head-surface-based positioning systems.

Analysis

Unambiguously illustrated 10/10 system

Currently, there are several different branches and derivatives of the 10/20 system, which tend to be used without clear definitions. Comparing different derivatives is something of a paradox: there is no unambiguous standard system, yet we must deal with the variability of the derivatives. As a practical compromise, we will first present the "unambiguously illustrated (UI) 10/10 system" as an unambiguous standard. This is not a new invention of ours, rather we simply eradicated ambiguity in the original description and complemented the 10/10 system that was proposed by ACNS (Klem et al., 1999), which is highly compatible with the one proposed by IFCN (Nuwer et al., 1998).

Here we will present a sufficiently unambiguous description for setting UI 10/10 positions and add detailed descriptions and related issues later, in appropriate contexts. We begin with setting four distinct primary reference points on the scalp anatomy: nasion (Nz), a dent at the upper root of the nose bridge; inion (Iz), an external occipital protuberance; left preauricular point (LPA), an anterior root of the center of the peak region of the tragus; and right preauricular point (RPA) determined as for the left (Fig. 1a). In the UI 10/10 system, LPA and RPA are the same as T9 and T10.

Next, we move on to setting reference curves on a scalp. For clarity, we define the term "reference curve" as a path of intersection between the head surface and a plane defined by three given points. First, we tentatively set the sagittal central reference curve using Nz and Iz, with Cz being temporarily defined as their midpoint, along the head surface (Fig. 1b). Second, we set the coronal central reference curve along LPA, Cz, and RPA by adjusting the sagittal central reference curve so that Cz equidistantly divides both the sagittal and coronal central reference curves (Fig. 1c). The sagittal central reference curve thus determined in the UI 10/10 system is divided from Nz to Iz, in 10% increments to generate Fpz, AFz, Fz, FCz, Cz, Cpz, Pz, POz, and Oz (Fig. 1d). Furthermore, the thus determined coronal central reference curve is divided in 10% increments from LPA to RPA in order to generate T7, C5, C3, C1, Cz, C2, C4, C6, and T8 (Fig. 1e).

Then, we set a left 10% axial reference curve along Fpz, T7, and Oz (Fig. 1f). For the left anterior quarter, we divide this portion of the curve by one fifth increments, from Fpz to T7, to set Fp1, AF7, F7, and FT7 (Fig. 1h). For the left posterior quarter, we divide by one fifth increments, from T7 to Oz, to set TP7, P7, PO7, and O1 (Fig. 1i). We do the same for the right hemisphere (Fig. 1g).

Next, we set six coronal reference curves. Since anterior–frontal (AF) and posterior–occipital (PO) reference curves follow slightly different rules, we first deal with four coronal reference curves in the middle, taking the frontal (F) coronal reference curve as an example. We define the F coronal reference curve using F7, Fz, and F8 (Fig. 1j). We divide the F7–Fz portion of the curve by one fourth increments, from F7 to Fz, to generate F5, F3, and F1 (Fig. 1k). We do the same for the F8–Fz portion on the right hemisphere (Fig. 1l). We apply the same quarterly division rule on each hemisphere to the fronto-central/temporal (FC/FT), temporo-/centro-parietal (TP/CP), and parietal (P) coronal reference curves (Fig. 1m). Next, we determine the anterior–frontal (AF) coronal reference curve using AF7, AFz, and AF8 (Fig. 1n). Since quarterly division results in overcrowded positions, the AF7–AFz portion of the curve is only bisected to generate AF3, and the AFz–AF8 portion, to generate AF4. Similarly, we work on the parieto-occipital (PO) coronal reference curve to set PO3 and PO4.

Finally, we set a left 0% axial reference curve along Nz, LPA (T9), and Iz (Fig. 1o). For the left anterior quarter, we divide by one fifth increments, from LPA (T9) to Nz, to set FT9, F9, AF9, and N1 (Fig. 1p; Klem et al., 1999). For the left posterior quarter, we divide by one fifth increments, from LPA (T9) to Iz, to set TP9, P9, PO9, and I1 (Fig. 1q). We do likewise for the right hemisphere to set N2, AF10, F10, FT10, TP10, P10, PO10, and I2.

For EEG studies, A1 and A2 electrodes are placed on the left and right ear lobes, but they are not important for other transcranial modalities. To maintain inter-modal generality, we do not deal with A1 and A2 in the current study.

In this way, we determined 81 positions (excluding A1 and A2) of the UI 10/10 systems with our best effort to exclude any ambiguity (Fig. 1r; circled points in Fig. 6 and in Supplementary

material 1). These 81 positions include all the positions described in the 10/10 system proposed by ACNS. We use the UI 10/10 system as the standard for inter-system comparison in the rest of the study.

The UI 10/10 system basically provides backward compatibility to the 10/20 system by Jasper (1958) except for the following differences. There are minor changes in nomenclature: T3, T4, T5, and T6 in the 10/20 system are renamed T7, T8, P7, and P8 respectively in the 10/10 system (Klem et al., 1999). The 10/20 system includes Pg1 and Pg2 placed on the pharynges. Since they are extremely hard to describe statistically, we excluded them from the analysis. The original 10/20 system by Jasper (1958) includes Cb1 and Cb2, which are supposed to be on the scalp above the cerebellum. To maintain backward compatibility, we excluded them from the UI 10/20 system. Thus, we defined 19 positions in the UI 10/20 system, excluding A1, A2, Pg1, Pg2, Cb1, and Cb2 (black circles in Fig. 6 and in Supplementary material 1).

Terminology regarding 10/20-derived systems

Currently, there are several different branches and derivatives of the 10/20 system, which tend to be used without clear definitions. In order to avoid any confusion in this study, we will clarify the terminology regarding the major variations of the 10/20 system. The sources that we used in our determination are summarized in Table 1. By "Jasper's 10/20" system, we refer to the 10/20 system that was described by Jasper (1958). We refer to the original ACNS definition as the "ACNS 10/10 system". We call the 10/10 system proposed by the IFCN the "IFCN 10/10 system" (Nuwer et al., 1998). It is basically the same as the ACNS 10/10 system except for the following differences: the IFCN 10/10 system prefers Jasper's original nomenclature, T3, T5, T4, and T6, rather than T7, P7, T8, and P8 as in the ACNS 10/10 system; the IFCN 10/10 system describes only 10/10 positions on or above the 10% axial reference curves albeit it does not exclude the possibility of using 10/10 positions on the 0% axial reference curve. When we do not have to distinguish between them, we call them collectively the "ACNS/IFCN 10/10 system". Chatrian et al. (1985) was the first to describe the 10/10 system, but we refer to it as "Chatrian's 10/10" system as their method is slightly different from the ACNS/IFCN and UI 10/10 systems (see Supplementary material 2 for detailed description). As described in the previous section, we define the "UI 10/10 system" as an unambiguous complementation for the 10/10 system proposed by ACNS (Klem et al., 1999). In addition, as described above, the UI 10/20 system was defined so that all the positions were included in

the UI 10/10 system. Oostenveld and Praamstra (2001) proposed the 10/5 system, which we refer to as "Oostenveld's 10/5" system, but we also use the term "Oostenveld's 10/10" system when specifically selecting 10/10 positions from among Oostenveld's 10/5 positions. Other variations will be discussed below.

Subjects and data analysis

We reanalyzed the MRI data sets of the 17 healthy volunteers (mongoloid; 9 males, 8 females; aged 22 to 51 years) with informed consent, which we had subsequently registered in the MNI coordinate system in a previous study (Okamoto et al., 2004a). Detailed methods for image processing, transformation to the MNI space, and virtual-head-surface landmark measurements were as previously described (Jurcak et al., 2005).

Briefly, we extracted head and brain images from the MRI data sets of the 17 subjects to produce isotropic images of $1 \times 1 \times 1$ mm voxels in size containing 8-bit continuous-tone data. These were subsequently converted to 2-bit data. The 10/20, 10/10, and 10/5 positions were determined according to the distance between landmarks over the head surface. Basically, we calculated the distance between a set of points over the head surface in a virtual space by defining a plane using three landmark positions. We extracted head surface points which comprised a cross-section between the plane and the head surface and drew a reference curve utilizing the extracted points. When only two points are given, we used the shortest distant search algorithm. This sets numerous planes intersecting the two points. Among the cross-sections between the planes and the head surface, we chose the one that gave rise to the shortest path along the head surface.

After multi-subject data for a given landmark position was expressed in MNI space, we calculated the mean coordinate locations across subjects as,

$$(\bar{x}, \bar{y}, \bar{z}) = \left(\frac{\sum x}{n}, \frac{\sum y}{n}, \frac{\sum z}{n}\right),$$

and the standard deviation (SD) as

$$SD = \sqrt{\frac{\sum(x - \bar{x})^2 + \sum(y - \bar{y})^2 + \sum(z - \bar{z})^2}{n - 1}},$$

where n is the number of subjects, and x, y, and z are MNI coordinate values for a given landmark point of a subject. The

Table 1
The number of standard positions in various 10/20-derived systems

System	Number of standard positions	Additional implicated positions	The most reliable source
Jasper's 10/20	19 (25 if A1, A2, Cb1, Cb2, Pg1, and Pg2 are included)	Nz, Iz, right and left preauricular points, Fpz, Oz, C5, C6, (A1, A2, Cb1, Cb2, Pg1, Pg2)	Fig. 6 in Jasper (1958)
Chatrian's 10/10	81	Right and left preauricular points	Figs. 1 and 2 in Chatrian et al. (1988)
IFCN 10/10	64	Iz, right and left preauricular points, electrode positions on and below 0% axial reference curve	Fig. 1 in Nuwer et al. (1998)
ACNS 10/10	75		Fig. 7 in Klem et al. (1999)
Oostenveld's 10/20	21		Fig. 1 in Oostenveld and Praamstra (2001)
Oostenveld's 10/10	85		Fig. 1 in Oostenveld and Praamstra (2001)
Oostenveld's 10/5	320	Nine positions that may interfere with the eyes	Fig. 2 in Oostenveld and Praamstra (2001)
UI 10/20	19		Fig. 6 of this manuscript
UI 10/10	81		Fig. 6 of this manuscript
UI 10/5	329		Fig. 6 of this manuscript

mean coordinate location provides the most likely estimates of the given point. Meanwhile, SD provides the measure for its variability across subjects within a given system and can be called inter-subject or intra-system variability, depending on the context.

Primary reference points

The original 10/20 system, at the time of its invention, was primarily intended for placing a relatively small number of electrodes in a balanced, reproducible manner over the scalp (Jasper, 1958). The description was only fine enough to support sparse electrode placement with accuracy in the order of centimeters.

10/20 measurement starts with setting four distinct primary reference points on the scalp anatomy, but the definitions of these reference points themselves are somewhat ambiguous. Among them, nasion, a dent at the upper root of the nose bridge, is the clearest and can easily be detected precisely. Inion, an external occipital protuberance, is less visible. Even if the structure is distinct enough, it is felt as a patch with a diameter of only several millimeters. For some subjects, the structure is often undetectable and an experimenter has to estimate its location from neighboring anatomical structures such as trapezius muscles.

Preauricular points are also a source of ambiguity. According to Jasper's original description, they were defined as depressions at the root of the zygoma just anterior to the tragus (Jasper, 1958). However, it is difficult to pinpoint the root of the zygoma at the skin, and the size of the tragus is approximately 1 cm. These factors make a precise, reproducible detection of the preauricular points difficult. Some laboratories have resolved this ambiguity with minor adjustments of their own. For example, when MR images of a subject are available, an external ear canal provides a stable anatomical guide. Another popular modification is the center of the peak region of the tragus, which is obvious for most subjects. As far as we know, the most stable local definition seems to be the dent between the upper edge of the tragus and the daith, which can be identified as a small point. Thus, for the preauricular points, we used four different definitions: the upper limit of the external ear canal, the center of the peak region of the tragus, the dent between the upper edge of the tragus and the daith, and, as a minor modification of Jasper's rather ambiguous definition, we tentatively restricted the preauricular region to the point located at the anterior root of the center of the peak region of the tragus, which can be detected in MR images. We used the same definition for the UI 10/10 system. In the rest of the current study, we will use this definition of preauricular points unless stated otherwise.

We first tested the inter-subject variability of these reference points by transferring them onto the MNI space and performing a group analysis. It should be noted that the variability includes the following two inseparable error sources: the structural differences of the external landmarks among individuals, and human error when detecting them manually. As Fig. 2 shows, the location of the nasion was almost invariant, while that of the inion had a larger standard deviation. These variabilities are intrinsic limitations in the accuracy of 10/20-derived systems and inevitable. The four local definitions of preauricular points lead to slightly different locations, but their precision in terms of standard deviations was almost the same.

Difference in the preauricular locations also affected the locations of other UI 10/10 positions. As Fig. 3 shows, temporal

10/10 positions near ears were largely affected by differences in the preauricular definitions. Deviation decreased in anterior, posterior, and parietal directions so that the 10/10 positions on prefrontal, parietal, and occipital regions were almost unaffected.

Sagittal central reference curve

After the four primary reference points (the nasion, the inion, and the preauricular points) are set, the sagittal central reference curve between Nz and Iz is determined. The original description of the 10/20 system proceeds to the determination of sagittal central reference curve immediately after primary reference point determination (Jasper, 1958). This process is equivalent to defining a curve in a three-dimensional area with only two points, and theoretically is not valid. One more rule is necessary. Therefore, Oostenveld and Praamstra (2001) suggested a readjustment of the tentatively drawn sagittal central reference curve so that Cz, or a point equidistant from both Nz and Iz, is also located at a point equidistant from the two preauricular points in order to maintain inter-hemispheric balance. The addition of Cz to Iz and Nz enabled the formation of a plane, and its intersection with the scalp yielded a unique sagittal central reference curve. Our virtual 10/20 determination program adopted the same adjustment procedure (Jurcak et al., 2005). The ACNS/IFCN 10/10 system inherits the sagittal central reference curve definition ambiguity of Jasper's 10/20 system (Jasper, 1958; Klem et al., 1999; Nuwer et al., 1998), but in the UI 10/10 system used in this study, we applied inter-hemispheric balancing. In all branches of 10/10 systems, the sagittal central reference curve thus determined is divided from Nz to Iz in 10% increments to generate Fpz, AFz, Fz, FCz, Cz, Cpz, Pz, POz, and Oz.

Coronal central reference curve

In Jasper's definition, the coronal central reference curve is on the plane made by the preauricular points and Cz (Jasper, 1958). The ACNS 10/10 system divides the coronal central reference curve in 10% increments from the left preauricular point (T9) to the right (T10) in order to generate T7, C5, C3, C1, Cz, C2, C4, C6, and T8, and thus we implemented the same strategy in the UI 10/10 system.

In contrast, Oostenveld and Praamstra (2001) used a different process. After determining the preauricular points (labeled LPA and RPA, equivalent to T9 and T10 respectively in the UI 10/10 system), an initial central coronal curve LPA–Cz–RPA is used to set points 10% above the preauricular points. In the current study, we tentatively designate them as pseudo-T7 and pseudo-T8 (equivalent to T7 and T8 in the UI 10/10 system). On the left hemisphere, a 10% horizontal reference curve was determined by a plane defined by Fpz, pseudo-T7, and Oz. Along this horizontal curve, T7 was set as a point equidistant from Fpz and Oz. The same process was applied to the right hemisphere to determine T8. Next, a coronal central reference curve was defined by a plane defined by T7, Cz, and T8 (Oostenveld's T7 and T8 are not necessarily identical to the UI T7 and T8, i.e., Oostenveld's pseudo-T7 and -T8). Finally, the contour was bisected in halves and points C5, C3, C1, and C6, C4, C2 were determined on each hemisphere at the quarter points of T7–Cz and T8–Cz respectively.

This method may not seem as straightforward as the UI method, but it stands on a carefully considered practical compromise. Jasper's 10/20, ACNS/IFCN 10/10, and the UI 10/10 systems are

Fig . 1.

mainly dependent on the central sagittal, central coronal, and 10% axial reference curves. However, we can only choose two reference curves to achieve equidistance divisions because the scalp is not symmetric. Though not mentioned explicitly, Jasper's 10/20 and ACNS/IFCN 10/10 systems divide the sagittal and coronal central reference curves at 50%. This inevitably results in an unbalanced division of the 10% axial reference curve, namely the distances Fpz-T7, Fpz-T8, Oz-T7, and Oz-T8 may differ. In contrast, Oostenveld's 10/10 system divides the sagittal and 10% axial reference curves at 50%. This results in equality in the lengths between Iz–Cz and Nz–Cz, Fpz–T7 and Oz–T7, and Fpz–T8 and Oz–T8, while the lengths between T7–Cz and T8–Cz may differ. However, the angles formed by T7, Cz, and pseudo-T7, and T8, Cz, and pseudo-T8 are small. Given that Cz to pseudo-T7 and Cz to pseudo-T8 distances are the same, Cz to T7 and Cz to T8 distances are also virtually the same. Therefore, Oostenveld's 10/10 system can place the landmark points on the three reference curves in a more balanced manner than the UI 10/10 system.

However, since the stability of Oostenveld's 10/10 system has only been implied, we evaluated it using virtual scalp measure-

Fig . 2.

Table 2
Length differences of reference curves between Oostenveld's and the UI 10/10 definitions

Reference curves	Oostenveld's definition	UI definition
Sagittal	Nz–Cz–Iz,	Nz–Cz–Iz,
	Nz–Cz (50%), Iz–Cz (50%)	Nz–Cz (50%), Iz–Cz (50%)
	By definition	By definition
Coronal	T7–Cz–T8	LPA–Cz–RPA
	T7–Cz (49.85±0.23%),	LPA–Cz (50%),
		RPA–Cz (50%)
	T8–Cz (50.15±0.23%)	By definition
Axial	Fpz–T7–Oz and	Fpz–T7–Oz and
	Fpz–T8–Oz	Fpz–T8–Oz
	Fpz–T7 (50%), Oz–T7 (50%)	Fpz–T7 (49.73±1.45%)
	Fpz–T8 (50%), Oz–T8 (50%)	Oz–T7 (50.27±1.45%)
	By definition	Fpz–T8 (49.55±1.39%)
		Oz–T8 (50.45±1.39%)

Values are presented in percentages with standard deviations (if applicable).

ments on the MR images of 17 subjects. As shown in Table 2, Oostenveld's system realized well-balanced divisions of the central coronal reference curve with a standard deviation six times lower than those of axial divisions of the UI system.

Moreover, we examined the locations of coronal central points determined by the UI and Oostenveld's 10/10 systems and their subsequent influences on other 10/10 positions. The two methods returned nearly identical results for all 10/10 positions (Supplementary material 3). As predicted theoretically, intra-system variability associated with the estimation was slightly lower in Oostenveld's 10/10 system, reflecting its higher precision. However, the differences are small enough to be negligible in most practical situations.

We also explored Oostenveld's 10/10 system's tolerance regarding the selection of preauricular reference points, which are only used tentatively to set the amplitude of T7 and T8. Preauricular points defined as the upper limit of an external ear canal, the center region of the tragus, and the anterior root of the tragus returned almost identical results for all 10/10 positions (Supplementary material 4). The dent between the upper edge of the tragus and the daith resulted in a slight upward shift. Thus, Oostenveld's 10/10 system is tolerant of variation in preauricular points in horizontal directions. When all of this is taken together, we demonstrated that Oostenveld's 10/10 system is optimized for setting a stable central coronal reference curve.

10% axial reference curve

Setting the 10% axial reference curve can also affect the location of 10/20, 10/10, and 10/5 positions. Theoretically, there are two ways of drawing two axial reference curves: working on anterior and posterior halves or on each hemisphere. In the original description of the 10/20 system by Jasper (1958), hemispheric division was implied. Oostenveld's 10/5 system clearly discussed and applied hemispheric division. To maintain backward compatibility with Jasper's 10/20 system, we adopted hemispheric division in the UI 10/10 system in this study.

On the other hand, Le et al. (1998) used anterior/posterior division to develop an automatic 10/20 guidance method. We also introduced anterior/posterior division primarily because the probabilistic registration methods we developed do not necessarily use all of the 10/20 reference points, hence often those on the anterior or posterior half were sufficient (Jurcak et al., 2005; Singh et al., 2005).

In hemispheric division, the 10% axial reference curve on the left hemisphere is defined by Fpz, T7, and Oz, and that on the right by Fpz, T8, and Oz. This leads to Fpz, Fp1, AF7, F7, FT7, T7, TP7, P7, PO7, O1, and Opz aligning on the same plane of the left hemisphere, and Fpz, Fp2, AF8, F8, FT8, T8, TP8, P8, PO8, O2, and Opz on that of the right. In anterior/posterior division, the 10%

Fig. 1. Landmark setting procedures for the UI 10/10 system. (a) Primary reference points. We set four primary reference points: inion (Iz), nasion (Nz), and preauricular points (LPA/T9 and RPA/T10). (b) Sagittal reference curve setting. We draw the sagittal central reference curve and bisect it to set Cz. At this stage, the setting is only tentative. (c) Central coronal reference curve setting and Cz adjustment. We draw the central coronal reference cure and adjust the location of Cz so that it bisects both sagittal and central coronal reference curves. (d) Determination of the landmarks on the sagittal reference curve. The landmarks are set at 10% increments. (e) Determination of the landmarks on the central coronal reference curve. The landmarks are set at 10% increments. (f) Determination of the 10% axial reference curve on the left hemisphere. It is set so that Fpz, T7, and Oz align on a plane. (g) Determination of the 10% axial reference curve on the right hemisphere. It is set so that Fpz, T8, and Oz align on a plane. (h) Determination of the landmarks on left anterior portion of the 10% axial reference curve. The landmarks are set at one fifth increments. The right anterior portion (not shown) is similar. (i) Determination of the landmarks on the left posterior portion of the 10% axial reference curve. The landmarks are set at one fifth increments. The right posterior portion (not shown) is similar. (j) Coronal reference curve setting. The frontal (F) coronal reference curve is shown. We draw it so that F7, Fz, and F8 align on a plane. (k) Determination of the landmarks on the left half portion of the coronal reference curve. The F coronal reference curve is shown. The landmarks are set at one fourth increments. (l) Determination of the landmarks on the right half portion of the coronal reference curve. The F coronal reference curve is shown. The landmarks are set at one fourth increments. (m) Determination of the landmarks on the coronal reference curves. As in the F coronal reference curve, fronto-central/temporal (FC/FT), temporo-/centro-parietal (TP/CP), and parietal (P) coronal reference curves and the landmarks on them are set. (n) Determination of the anterior–frontal (AF) and parieto-occipital (PO) coronal reference curves and landmarks. For each hemisphere, AF and PO reference curves are only bisected to produce landmarks. (o) Determination of the 0% axial reference curve on the left hemisphere. It is set so that Nz, LPA (T9), and Iz align on a plane. The right hemisphere (not shown) is similar. (p) Determination of the landmarks on the left anterior portion of the 0% axial reference curve. The landmarks are set at one fifth increments. The right anterior portion (not shown) is similar. (q) Determination of the landmarks on the left posterior portion of the 0% axial reference curve. The landmarks are set at one fifth increments. The right anterior portion (not shown) is similar. (r) All UI 10/10 points are set. The right hemisphere (not shown) is similar.

Fig. 2. Locations of primary reference points. All positions are overlaid on the normalized and averaged head surface images of 17 subjects. MNI coordinates are also shown. L and R represent left and right, respectively. The centers of the circles represent the most likely locations of MNI coordinates for the primary reference points. The edges represent the boundaries defined by standard deviation. Nasion and inion are shown as green circles. Preauricular points are shown as: blue for the anterior root of the tragus, yellow for the peak region of the tragus, black for the external ear canal, and red for the point determined between the upper edge of the tragus and the daith. (A) Frontal view. (B) Occipital view. (C) Left temporal view. (D) Schematic of an ear showing the four definitions of preauricular points used in this study: the anterior root of the tragus (blue dot), the peak region of the tragus (yellow dot), the upper limit of the external ear canal (black dot), and the point determined between upper edge of the tragus and the daith (red dot).

axial reference curve is defined by T7, Fpz, and T8 on the anterior half, and T7, Oz, and T8 on the posterior half. This leads to T7, Ft7, F7, AF7, Fp1, Fpz, Fp2, AF8, F8, FT8, and T8 aligning on the same plane on the anterior half, and T7, TP7, P7, PO7, O1, Opz O2, PO8, P8, TP8, and T8 on the posterior half.

It should be noted that Jasper's 10/20 system was further ambiguous in setting the reference points on the 10% axial reference curve (Jasper, 1958). From Fpz to Oz, Jasper suggested setting the reference points at 10, 30, 50, 70, and 90% distances, but since Fpz–T7 and T7–Oz distances could not be equal, this was theoretically impossible. Consequently, researchers should either neglect small differences for rough measurements or work on each quarter. To avoid such inconsistency, we chose to work on each quarter in the UI 10/10 system, and also in the anterior/posterior division used in this study. Namely, each Fpz–T7, T7–Oz, Oz–T8, and T8–Fpz portion of 10% axial reference curves was divided in one fifth increments to generate 10/10 positions.

We examined how hemispheric and anterior/posterior divisions affect the locations of reference points on 10% axial reference curves. As Fig. 4 shows, the hemispheric division resulted in slightly lower 10/10 positions on lower parts of the scalp especially those on 10% and 0% axial reference curves. Thus, there are non-negligible inter-system differences between 10/10 positions determined by hemispheric and anterior/posterior divisions. However, intra-system variability associated with the estimation was at similar levels.

Coronal reference curves

In the original description of the 10/20 system by Jasper (1958), mid-frontal and mid-parietal positions (F3, F4, P3, and P4) seemed, according to our best estimation, to be located on the coronal reference curve along planes defined by F7, Fz, and F8, and P7, Pz, and P8. Therefore, in the UI 10/10 system, we set coronal reference curves along planes defined by three points. However, this definition is difficult to realize practically without extreme precision when measuring the scalp. As far as we have observed, experimenters tend to locate mid-frontal and mid-parietal positions slightly below the exact coronal curve. Thus, in our former study, we mimicked this human measurement by

setting F3 at the middle of the shortest-distance curve between F7 and Fz (Jurcak et al., 2005). This tendency seems more obvious when setting AF7–AFz–AF8 and PO7–POz–PO8 coronal reference curves for the 10/10 system.

Fig. 5 shows 10/10 standard positions defined by the two definitions of the coronal reference curves described above. Intra-system variability was bigger when coronal curves were defined by the shortest-distant method. There was also an obvious shift where the shortest-distant method tended to locate anterior points further anterior, and posterior points further posterior.

Oostenveld's 10/5 system

As demonstrated above, provided that the choices of the primary reference points and reference curves are clear enough, 10/20 and 10/10 systems can set precise and reproducible scalp landmarks. The next question is how far the system can be extended. To date, a 10/5 system with more than 300 distinct scalp landmarks has been proposed (Oostenveld and Praamstra, 2001), but there is the possibility of excessive landmark setting. Therefore, we examined the variability of 10/5 positions for multi-subject studies by performing virtual 10/5 measurements on the MR images of 17 subjects. The measurements were kept as close as possible to the original description by Oostenveld and Praamstra (2001).

Nomenclature for the 10/5 standard positions is presented in Supplementary material 5. Briefly, the central sagittal, coronal, and 10% axial reference curves were drawn as in Oostenveld's 10/10 system, described above. On the central sagittal and 10% axial reference curves, 10/5 standard positions were set at 5% intervals. Exceptions to this rule were the anterior and posterior 5% points on 10% axial reference curves, which Oostenveld and Praamstra did not describe clearly. We designated these points as Fp1h, Fp2h, O1h, and O2h by extending their logic on the 10% axial curve. The point between Nz and Fpz was designated as NFpz and nearby points on the 5% axial curve designated as NFp1h and NFp2h. On the central coronal curve on the T7–Cz–T8 plane, we worked on each hemisphere separately setting 10/5 standard positions at 12.5% intervals between T7 and Cz and repeating the same procedure on the right hemisphere. For other coronal reference curves posterior to AFp and anterior to POO, we used the same

Fig. 3. Effects of primary reference point selection on the location of the UI 10/10 positions. All positions were overlaid on the normalized and averaged head surface images of 17 subjects. MNI coordinates are also shown. The centers of the circles represent the most likely locations of MNI coordinates for 10/20 standard positions. The edges represent the boundaries defined by standard deviation. Nasion and inion are shown as green circles. Preauricular points are shown as: blue for the anterior root of the tragus; yellow for the peak region of the tragus; black for the external ear canal; red for the point determined between the upper edge of the tragus and the daith. Color for 10/10 locations depends on the preauricular point selection. The UI 10/10 positions that are not virtually affected are shown in pink. The asterisks indicate 10/10 positions that can be on the eyes (i.e., N1, N2), and sharps indicate those on or beneath the ear lobes (i.e., TP9 and TP10). (A) Frontal view. (B) Occipital view. (C) Left temporal view. (D) Right temporal view. (E) Top view.

Fig. 4. Effects of the selection of 10% axial reference curves on the location of 10/10 positions. Basic descriptions of circles showing 10/10 positions, coordinates, and a scalp template are the same as in Fig. 3. Blue circles represent 10/10 positions after 10% axial reference curves were determined on each hemisphere defined by planes made by Fpz–T7–Oz and Fpz–T8–Oz points, according to the UI 10/10 system. Red circles represent 10/10 positions after 10% axial reference curves were determined on the anterior and posterior half defined by planes made by T7–Fpz–T8 and T7–Oz–T8 points. The UI positions that are not theoretically affected by the 10% axial reference curve selections are shown in pink. The asterisks and sharps indicate 10/10 positions that can be on the eyes, and on or beneath the ear lobes, respectively. (A) Frontal view. (B) Occipital view. (C) Left temporal view. (D) Right temporal view. (E) Top view.

Fig. 5. Effects of the selection of coronal curves on the location of 10/10 positions. Basic descriptions of circles showing 10/10 positions, coordinates, and a scalp template are the same as in Fig. 3. Blue circles represent points lying on the plane defined by two starting points on the 10% axial curve and one point on the sagittal reference curve, as determined according to the UI 10/10 system. Red circles represent points that lie on curves with the shortest distance between two corresponding points on the 10% axial reference curve and the sagittal central reference curve. Pink circles represent points on the central coronal, sagittal, and 10% axial reference curves that are not affected by the selection. The asterisks and sharps indicate 10/10 positions that can be on the eyes, and on or beneath the ear lobes, respectively. (A) Frontal view. (B) Occipital view. (C) Left temporal view. (D) Right temporal view. (E) Top view.
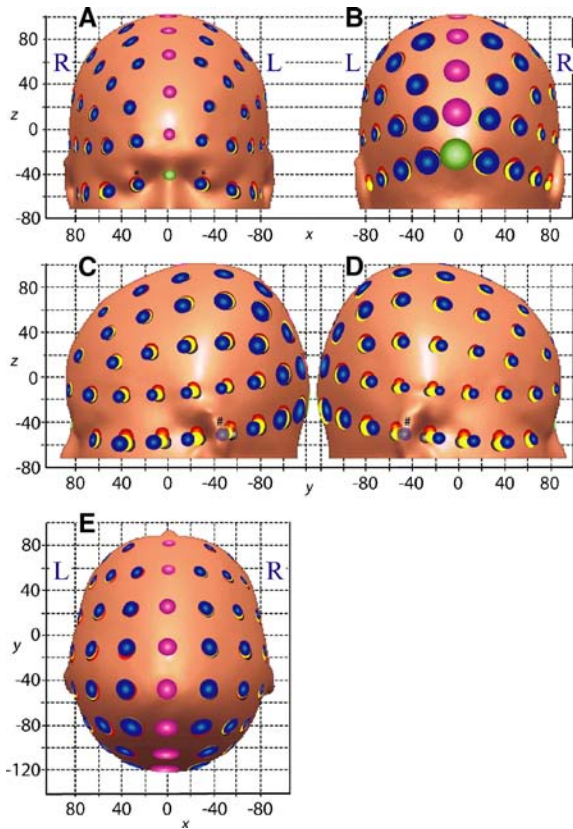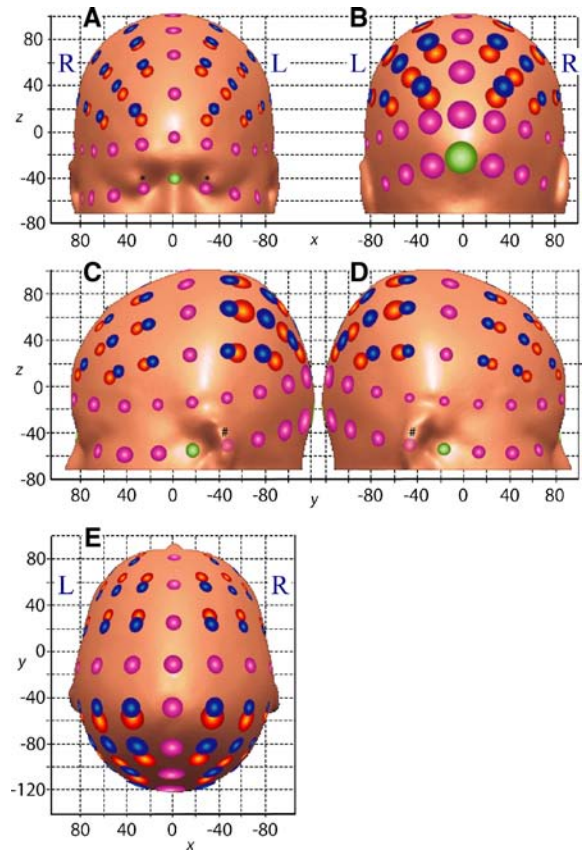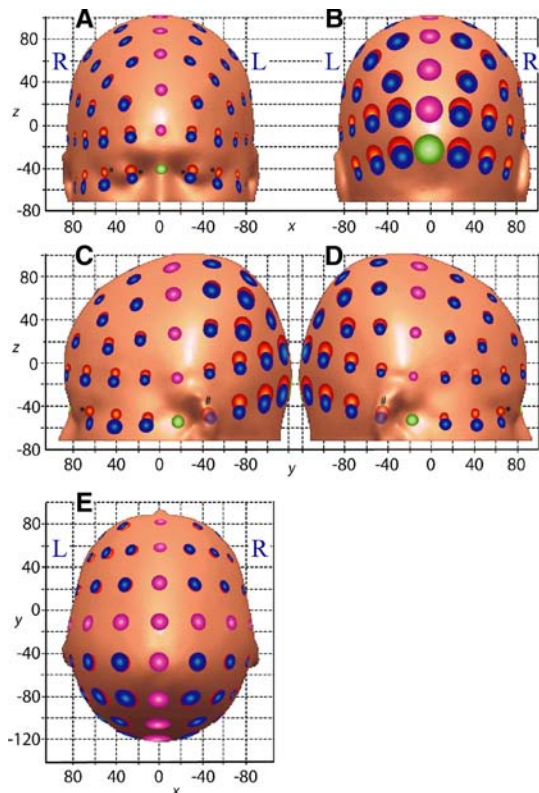
Fig . 3.

Fig . 5.

Fig . 4.

strategy as with the central coronal curve. AFp and POO coronal curves were drawn, but halfway points were omitted.

To our knowledge, there is no clear description for setting points on 0% and 5% axial reference curves. There were two possibilities: extending coronal reference curves dorsally or setting the 0% and 5% axial reference curves independently. Tentatively, we chose the latter strategy. We set a plane using Nz, LPA, and Iz on the left hemisphere, and 10/5 standard positions at 5% distances. However, anterior 5, 10, and 15% points are likely on the eyes. For the 5% axial curve, we set pseudo-T9h and pseudo-T10h 5% above the preauricular points from the distance LPA–Cz–RPA. Using NFpz, pseudo-T9h, and OIz, we set a plane and 10/5 standard positions at 5% distances. Again, anterior 10, 15, and 20% points are likely on the eye. We followed the same procedure with the right hemisphere. In this way, we estimated a total of 329 Oostenveld's 10/5 standard positions (including nine additional positions) and described their distribution on the MNI space (Supplementary material 6).

Unambiguously illustrated 10/5 system

Aside from some ambiguity, as mentioned above, we regard Oostenveld's 10/5 system as a well-designed derivative of the 10/20 system with emphasis on the balanced setting of central sagittal, central coronal, and 10% axial reference curves. However, it is possible in practical situations that researchers adopt the nomenclature of Oostenveld's 10/5 system but simply extend the ACNS/IFCN 10/10 system to the 10/5 system without readjusting the central coronal reference curve. Therefore, we will extend the

UI 10/10 system to cover 10/5 points and call it the UI 10/5 system (Fig. 6).

Assuming that all the UI 10/10 positions have been set properly, we set 10/5 positions on the central sagittal reference curve along LPA (T9), Cz, and RPA (T10) by 5% increments. Similarly, we set 10/5 positions on the central coronal reference curve along Nz, Cz, and Iz by 5% increments. For the 10% axial reference curve, since the lengths of its quarterly portions are different, we worked on each quarter and set 10/5 positions by one tenth increments. Next, we set a coronal reference curve by selecting two corresponding 10% axial points and one central sagittal reference point to define the coronal reference curve (e.g., AFF7, AFFz, and AFF8 for the AFF coronal reference curve) so that the three points are on the same plane. Since the lengths of the hemispheric portions of the curves may not be the same, we worked on each hemisphere separately, placing 10/5 positions by one eighth increments. However, to avoid over-crowded positioning on AFp and POO coronal reference curves, we worked on each hemisphere to place 10/5 positions by one fourth increments as in Oostenveld's 10/5 system. For the 0% axial reference curve, since the lengths of its

quarterly portions are different, we worked on each quarter and set 10/5 positions by one tenth increments. Finally, we set 5% reference curves on the left hemisphere so that NFpz, T9h, and OIz are on the same plane and did the same on the right hemisphere, using NFpz, T10h, and OIz. As in the cases of 0% and 10% axial reference curves, the lengths of the quarterly portions of the 5% axial reference curve are different. Thus, we work on each quarter and set 10/5 positions by one tenth increments. Consequently, we estimated a total of 329 UI 10/5 standard positions and described their variability on the MNI space (Fig. 7).

Validity of 10/20, 10/10, and 10/5 systems

Next, we examined whether landmark positions of 10/20, 10/10, and 10/5 systems could be resolved from neighboring positions. We measured the center-to-center distance between two neighboring positions (D) and compared it to the sum of the standard deviations of the two positions ($SD_1 + SD_2$). We regarded the two positions as separate when the distance between the two neighboring positions was larger (i.e., $D > SD_1 + SD_2$).
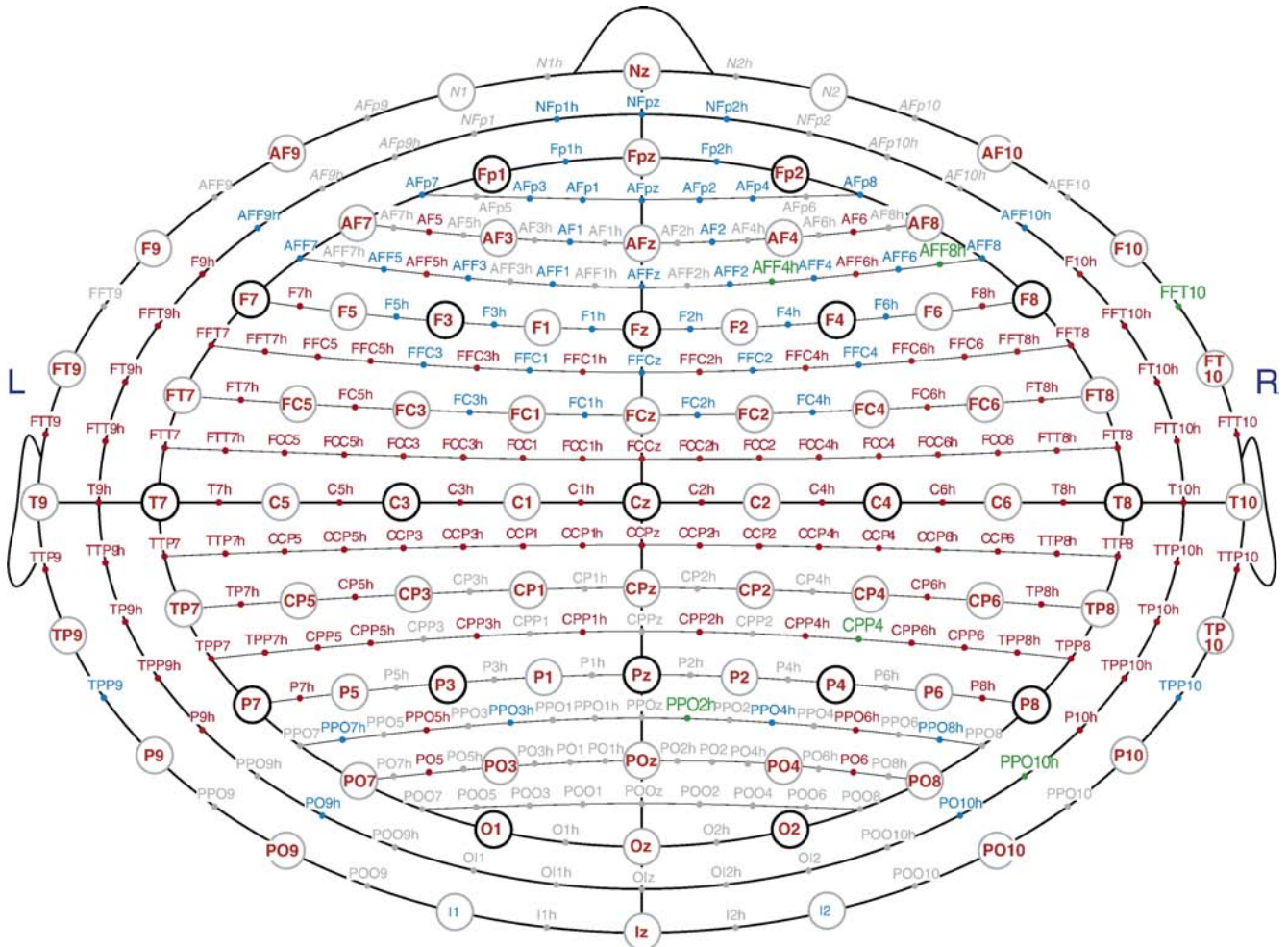

Fig. 6. The UI 10/5 system. Total number of points is 329 including 12 points, likely lying on the eyes (shown in gray italics). Black open circles indicate the UI 10/20 positions, gray open circles indicate additional positions introduced in the UI 10/10 system. Colored positions (red, blue, and green) are the points that can be set effectively on a scalp when neighboring positions are not allowed to overlap: 185 points preserving both anterior/posterior and right/left symmetries are in red, an additional 50 points preserving only right/left symmetry are in blue, and 6 more points that are just separated from the neighboring positions are in green. The rest of the UI 10/5 positions (76 points), which interfered with neighboring positions, are indicated in gray.
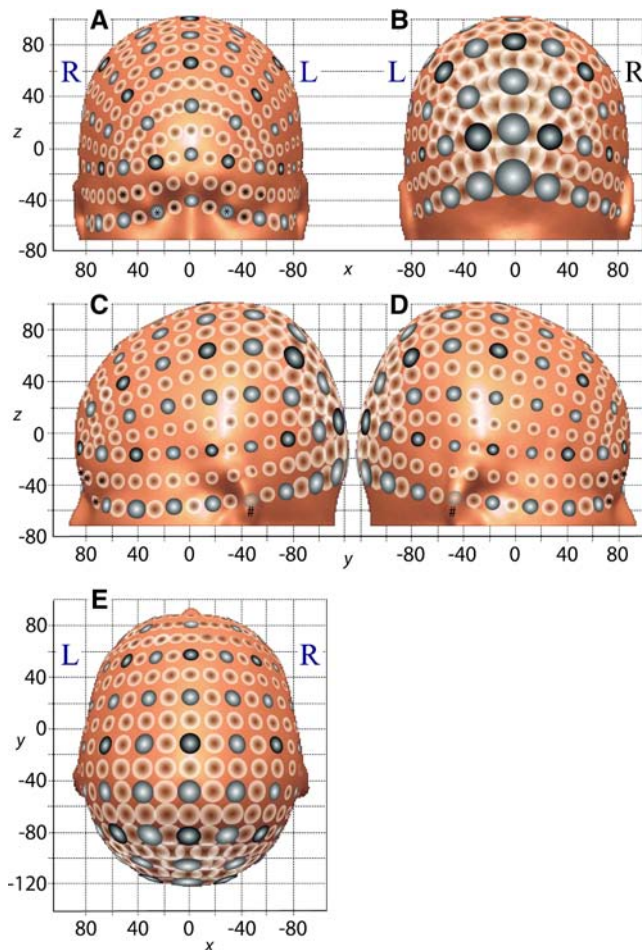
Fig. 7. Locations of the UI 10/5 standard positions (329) in MNI space and their spatial variability. MNI coordinates are also shown. The centers of the circles represent the most likely locations of MNI coordinates for 10/20 standard positions. The edges represent the boundaries defined by standard deviation. Black circles indicate the UI 10/20 positions (19), gray circles indicate the additional positions in the UI 10/10 system (62). The rest of the UI 10/5 positions (248) are indicated in white. The asterisks and sharps indicate positions that can be on the eyes, and on or beneath the ear lobes, respectively. (A) Frontal view. (B) Occipital view. (C) Left temporal view. (D) Right temporal view. (E) Top view.

A given 10/10 system provides backward compatibility to the corresponding 10/20 system for at least 19 standard positions. Thus, we extracted them from various branches of the 10/10 systems presented above. In all cases, the 10/20 standard positions were separated from each other.

We extended this analysis to 10/10 systems. First of all, in the UI 10/10 system, 81 positions were all separated from each other on a scalp in MNI space. Indeed, in all the other branches, 10/10 positions were separated from each other except for a marginal level of overlapping between PO3 and O1 as determined by a shortest-distant search method for coronal reference curve setting (Fig. 5). If we tolerate these negligible or minor exceptions, we can conclude that the UI 10/10 system provides stable and well-separated landmarks on the scalp.

We further examined whether the UI and Oostenveld's 10/5 positions could be resolved from neighboring positions. Since there were obviously overlapping positions, we eliminated the

more subordinate positions in the following order of preference: 10/20, 10/10, and 10/5 positions. Furthermore, we excluded 12 positions that interfere with the eyes.

For Oostenveld's 10/5 system, 241 points survived as distinct positions. In general, anterior positions were more clearly separated than posterior positions (Supplementary material 5). In order to set a maximum balanced separation to achieve right/left symmetry, we further eliminated six positions (Supplementary material 5). In addition to the right/left symmetry, we further sought anterior/posterior symmetry. Ultimately, 189 points survived. These positions may serve as a fair criterion for setting up scalp landmarks in Oostenveld's 10/5 system.

For the UI 10/5 system, the results were similar as for Oostenveld's 10/5 system. As Fig. 6 shows, 241 points survived as distinct positions. As in the case of Oostenveld's 10/5 system, anterior positions were more clearly separated than posterior positions. After applying the right/left symmetry criteria, 235 positions survived (Fig. 6). After further applying the anterior/posterior symmetry criteria, 185 positions survived. These positions may serve as a fair criterion for setting up scalp landmarks for the UI 10/5 system.

Discussion

The aim of the current study was to evaluate the effectiveness of 10/20-derived systems in the light of head-surface-based positioning systems. From the time of its invention as a method to set up EEG electrodes in a balanced reproducible way, the 10/20 system has gained importance as a standard method for setting landmarks over the scalp.

Nevertheless, the current definitions for the 10/20 system and its derivatives still remain ambiguous, and this reduces the potential accuracy of these systems. Ideally, in order to increase accuracy, the current definitions should be revised to provide more detailed methods for setting landmarks. However, in practice, it takes time to realize such standardizations. Even after standardization, it would take time for the new methods to become widely used. For example, the transition from Talairach to MNI stereotaxic coordinate systems (reviewed in Brett et al., 2002) is still in process. It is possible, of course, that this transition may never be fully completed and that researchers will ultimately opt for the coexistence of the two systems.

Therefore, we have chosen to present methods to probabilistically describe major branches of 10/20-derived systems. These variations may have developed to satisfy the individual needs of experimenters and clinicians and would therefore be useful in some situations. There were inter-system variabilities between 10/10 positions defined in different methods. Specifically, choice of hemispheric or anterior/posterior divisions and of coronal reference curves causes non-negligible differences in the locations of 10/10 positions. These observations clearly demonstrate the need to clarify which branch of 10/20-derived systems is used to set scalp landmarks in order to describe their locations explicitly. On the other hand, intra-system variabilities were at similar levels. From these observations, we conclude that, as long as a detailed rule for a particular method is provided, it will yield precise landmarks. In addition, we should stress here that we do not intend to judge which system is superior but to demonstrate that landmarks set by any system can be probabilistically described.

In the best case scenario, with a clear description of the rules of measurement, the 10/5 system can set as many as 329 positions on a scalp (Oostenveld and Praamstra, 2001). Full use of these

positions may be useful for EEG experiments, but such high density setting may result in overestimations for relative head surface positioning. When two neighboring positions are not allowed to overlap in terms of standard deviations, the number of effective 10/5 positions was reduced to 241 for Oostenveld's and UI 10/5 systems. Moreover, when they were balanced out for anterior/posterior and right/left symmetries, the number of effective 10/5 positions was reduced to 189 for Oostenveld's system and 185 for the UI 10/5 system. However, it would not be unrealistic to state that, with careful measurements, the 10/5 system is capable of providing more than 180 distinct landmarks on a scalp.

The criteria for separation used in this study, namely, non-overlapping of SD of neighboring positions, are only rough guidelines. There is the possibility of type I errors, where inseparable positions are judged as separable (see Supplementary 7 for the results of the Monte Carlo simulation for type I errors).

It is worthwhile mentioning that all 10/10 positions remained intact after the exclusion of overlapping points. In other branches of 10/10 systems also, most 10/10 positions, with only a few marginal exceptions, were well separated from each other. Thus, landmark setting according to a given 10/10 system can also be considered reliable as long as explicit definitions are provided.

The virtue of the current study would be most appreciated in the context of a cross-modal approach, which is now common in the neuroimaging community. Since there is no single perfect modality for assessing human brain function, ideally, data from different modalities should be integrated into a single common platform. In pursuit of a common arena for inter-modal assessment, there has been a movement described as a probabilistic approach to expressing all functional brain data as entries in a brain atlas that expands into space and time (Abbott, 2003; Mazziotta et al., 2000; Mazziotta et al., 2001a,b; Toga and Thompson, 2001). The probabilistic atlas per se has not been realized, but its philosophy has become widespread so that the essential concept for this integrative approach has already been realized. It is now common practice to present tomographic imaging data in stereotaxic standard coordinate systems such as Talairach or MNI coordinates (Talairach and Tournoux, 1988; Collins et al., 1994; reviewed in Brett et al., 2002). With respect to expressing the transcranial brain mapping data on MNI space, the current study will be beneficial for three major technical applications. First, the current data set will provide finer MNI coordinate estimation for EEG signal source elucidation (Pascual-Marqui et al., 2002). It is also plausible to elucidate the accuracy of the signal source estimation by applying error propagation law or resampling simulations (Singh et al., 2005; Tsuzuki et al., 2006). Second, the data set will be used as standard landmarks to guide fNIRS probes or a TMS coil on a scalp for reproducible measurements. The reliability of the selected landmarks can be evaluated by error information. Third, the data set will present more reference landmark positions to perform probabilistic registration of fNIRS and TMS data to standard stereotaxic space (Okamoto et al., 2004a; Okamoto and Dan, 2005; Singh et al., 2005). In theory, we can probabilistically register transcranial data without MR images with just four reference points, but inclusion of more reference points selected in a balanced way enhances the accuracy of the probabilistic registration.

The current study may also be viewed as part of retrospective trends in the neuroimaging community. In one direction, there are extensive cytoarchitectural and areal parcellation studies being undertaken to provide probabilistic anatomical basis for the MNI system (Eickhoff et al., 2005; reviewed in Amunts and Zilles, 2001). These works are considered to be a modern implementation of Brodmann's legendary works to describe the cytoarchitecture of the brain (Brodmann, 1908). In a different direction, we are seeking to re-establish Jasper's work in a modern perspective in order to create a link between stereotaxic coordinates and relative head-surface-based positioning systems. Such an approach would be beneficial for creating a tighter link between tomographic and transcranial brain mapping methods. Powered by old ideas, we believe that this study will accelerate the movement for cross-model data sharing and integration on a common platform.

Acknowledgments

Appendix A. Supplementary data

Supplementary data associated with this article can be found, in the online version, at doi:10.1016/j.neuroimage.2006.09.024.

References

Abbott, A., 2003. Neuroscience: a new atlas of the brain. Nature 424, 249–250.

American Electroencephalographic Society, 1994. Guideline thirteen: guidelines for standard electrode position nomenclature. American Electroencephalographic Society. J. Clin. Neurophysiol. 11, 111–113.

Amunts, K., Zilles, K., 2001. Advances in cytoarchitectonic mapping of the human cerebral cortex. Neuroimaging Clin. N. Am. 11, 151–169.

Brett, M., Johnsrude, I.S., Owen, A.M., 2002. The problem of functional localization in the human brain. Nat. Rev., Neurosci. 3, 243–249.

Brodmann, K., 1908. Beiträge zur histologischen Lokalisation der Großhirnrinde. VI: Die Cortexgliederung des Menschen. J. Psychol. Neurol. X, 231–246 (in German).

Chatrian, G.E., Lettich, E., Nelson, P.L., 1985. Ten percent electrode system for topographic studies of spontaneous and evoked EEG activity. Am. J. EEG Technol. 25, 83–92.

Chatrian, G.E., Lettich, E., Nelson, P.L., 1988. Modified nomenclature for the "10%" electrode system. J. Clin. Neurphysiol. 5, 183–186.

Collins, D.L., Neelin, P., Peters, T.M., Evans, A.C., 1994. Automatic 3D intersubject registration of MR volumetric data in standardized Talairach space. J. Comput. Assist. Tomogr. 18, 192–205.

Eickhoff, S.B., Stephan, K.E., Mohlberg, H., Grefkes, C., Fink, G.R., Amunts, K., Zilles, K., 2005. A new SPM toolbox for combining probabilistic cytoarchitectonic maps and functional imaging data. Neuro-Image 25, 1325–1335.

Herwig, U., Satrapi, P., Schonfeldt-Lecuona, C., 2003. Using the international 10–20 EEG system for positioning of transcranial magnetic stimulation. Brain Topogr. 16, 95–99.

Jasper, H.H., 1958. The ten–twenty electrode system of the International Federation. Electroencephalogr. Clin. Neurophysiol. 10, 367–380.

Jurcak, V., Okamoto, M., Singh, A., Dan, I., 2005. Virtual 10–20 measurement on MR images for inter-modal linking of transcranial and tomographic neuroimaging methods. NeuroImage 26, 1184–1192.

Klem, G.H., Luders, H.O., Jasper, H.H., Elger, C., 1999. The ten–twenty electrode system of the International Federation. The International Federation of Clinical Neurophysiology. Electroencephalogr. Clin. Neurophysiol., Suppl. 52, 3–6.

Le, J., Lu, M., Pellouchoud, E., Gevins, A., 1998. A rapid method for determining standard 10/10 electrode positions for high resolution EEG studies. Electroencephalogr. Clin. Neurophysiol. 106, 554–558.

Mazziotta, J.C., Toga, A.W., Evans, A.C., Fox, P., Lancaster, J., Woods, R., 2000. A probabilistic approach for mapping the human brain. In: Toga, A.W., Mazziotta, J.C. (Eds.), Brain Mapping: The System. Academic Press, San Diego, pp. 141–156.

Mazziotta, J., Toga, A., Evans, A., Fox, P., Lancaster, J., Zilles, K., Woods, R., Paus, T., Simpson, G., Pike, B., Holmes, C., Collins, L., Thompson, P., MacDonald, D., Iacoboni, M., Schormann, T., Amunts, K., Palomero-Gallagher, N., Geyer, S., Parsons, L., Narr, K., Kabani, N., Le Goualher, G., Boomsma, D., Cannon, T., Kawashima, R., Mazoyer, B., 2001a. A probabilistic atlas and reference system for the human brain: International Consortium for Brain Mapping (ICBM). Philos. Trans. R. Soc. Lond., B Biol. Sci. 356, 1293–1322.

Mazziotta, J., Toga, A., Evans, A., Fox, P., Lancaster, J., Zilles, K., Woods, R., Paus, T., Simpson, G., Pike, B., Holmes, C., Collins, L., Thompson, P., MacDonald, D., Iacoboni, M., Schormann, T., Amunts, K., Palomero-Gallagher, N., Geyer, S., Parsons, L., Narr, K., Kabani, N., Le Goualher, G., Feidler, J., Smith, K., Boomsma, D., Hulshoff Pol, H., Cannon, T., Kawashima, R., Mazoyer, B., 2001b. A four-dimensional probabilistic atlas of the human brain. J. Am. Med. Inform. Assoc. 8, 401–430.

Nuwer, M.R., 1987. Recording electrode site nomenclature. J. Clin. Neurophysiol. 4, 121–133.

Nuwer, M.R., Comi, G., Emerson, R., Fuglsang-Frederiksen, A., Guerit, J.M., Hinrichs, H., Ikeda, A., Luccas, F.J., Rappelsburger, P., 1998. IFCN standards for digital recording of clinical EEG. International Federation of Clinical Neurophysiology. Electroencephalogr. Clin. Neurophysiol. 106, 259–261.

Okamoto, M., Dan, I., 2005. Automated cortical projection of head-surface locations for transcranial functional brain mapping. NeuroImage 26, 18–28.

Okamoto, M., Dan, H., Sakamoto, K., Takeo, K., Shimizu, K., Kohno, S., Oda, I., Isobe, S., Suzuki, T., Kohyama, K., Dan, I., 2004a. Three-dimensional probabilistic anatomical cranio-cerebral correlation via the international 10–20 system oriented for transcranial functional brain mapping. NeuroImage 21, 99–111.

Okamoto, M., Dan, H., Shimizu, K., Takeo, K., Amita, T., Oda, I., Konishi, I., Sakamoto, K., Isobe, S., Suzuki, T., Kohyama, K., Dan, I., 2004b. Multimodal assessment of cortical activation during apple peeling by NIRS and fMRI. NeuroImage 21, 1275–1288.

Oostenveld, R., Praamstra, P., 2001. The five percent electrode system for high-resolution EEG and ERP measurements. Clin. Neurophysiol. 112, 713–719.

Pascual-Marqui, R.D., Esslen, M., Kochi, K., Lehmann, D., 2002. Functional imaging with low-resolution brain electromagnetic tomography (LORETA): a review. Methods Find. Exp. Clin. Pharmacol. 24 (Suppl. C), 91–95.

Singh, A.K., Okamoto, M., Dan, H., Jurcak, V., Dan, I., 2005. Spatial registration of multichannel multi-subject fNIRS data to MNI space without MRI. NeuroImage 27, 842–851.

Suarez, E., Viegas, M.D., Adjouadi, M., Barreto, A., 2000. Relating induced changes in EEG signals to orientation of visual stimuli using the ESI-256 machine. Biomed. Sci. Instrum. 36, 33–38.

Talairach, J., Tournoux, P., 1988. Co-Planar Stereotaxic Atlas of the Human Brain: 3-Dimensional Proportional System: An Approach to Cerebral Imaging. Thieme Medical Publishers, New York.

Toga, A.W., Thompson, P.M., 2001. Maps of the brain. Anat. Rec. 265, 37–53.

Tsuzuki, D., Jurcak, V., Singh, A.K., Okamoto, M., Watanabe, E., Dan, I., 2006. Virtual spatial registration of stand-alone fNRS data to MNI space. NeuroImage, doi:10.1016/j.neuroimage.2006.10.043.